Adaptive finite volume methods for sediment transport in porous media

Mohammed Seaid

School of Engineering, University of Durham, UK

Joint work with: Fayssal Benkhaldoun (Université Paris 13, France)

Saida Sari (Université Paris 13, France)




Objectives

- Numerical models can help to:
  - Understand the hydrodynamics budget
  - Predict the morphodynamics and sediment transport
  - Minimize the environmental damages
- Numerical models need:
  - A mathematical model for hydrodynamics
    (Navier-Stokes equations, shallow water equations ...)
  - A mathematical model for morphodynamics
    (Exner, advection-diffusion equations, ...)
  - A mathematical model for erosion and deposition of sediments
    (Empirical equations, particles, ...)
  - A numerical method for solution procedure
    (Finite element method, finite volume method, LBM ...)
  - Saptial and temporal scales ?

Outline

- Mathematical Models
  - Equations for water flow
  - Equations for sediment transport
- Numerical Method
  - Finite volume discretization
  - Formulation of the method
- Numerical Results
  - Verification and validation results
  - Dam-break over erodible sediment beds

I. Mathematical Models

Depth-averaged equations

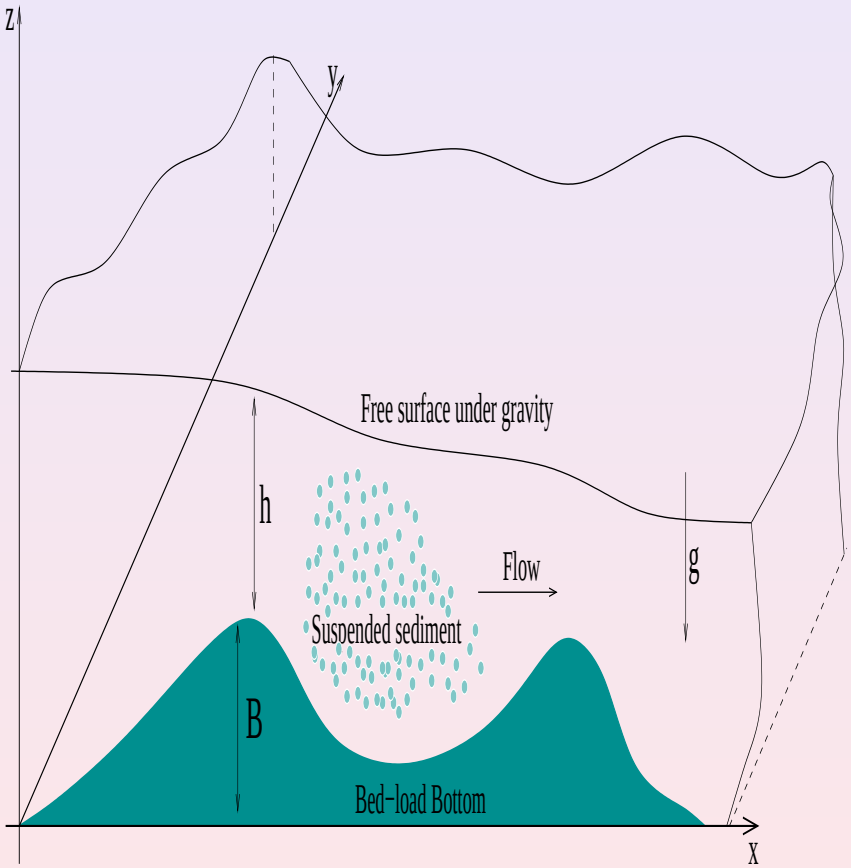

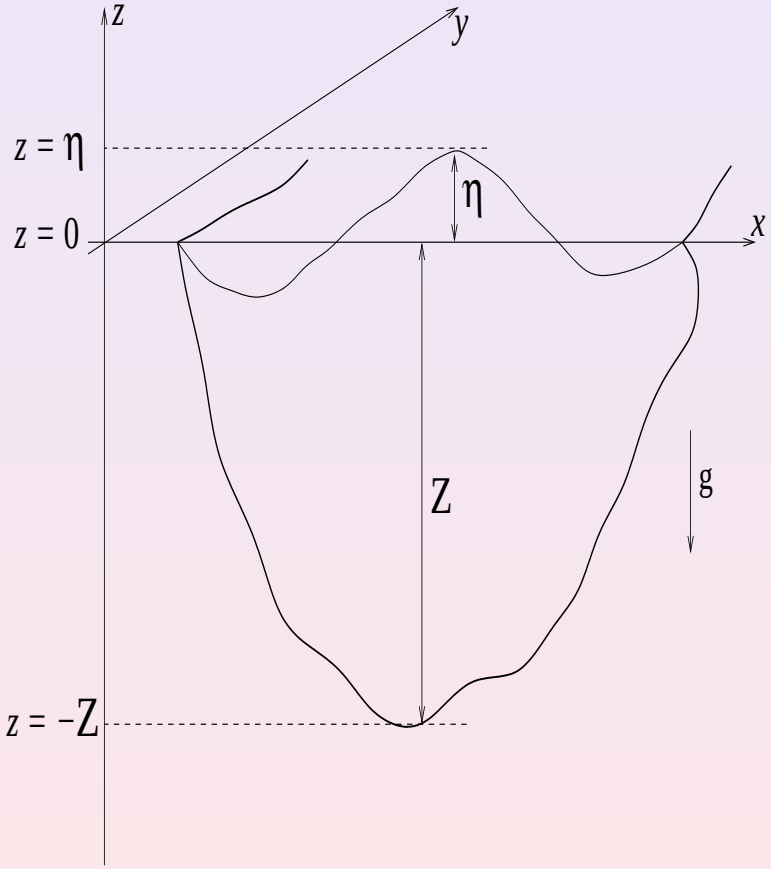

Shallow Water Equations

$$\partial_t h + \partial_x(hu) + \partial_y(hv) = \frac{E-D}{1-p},$$

$$\partial_t(hu) + \partial_x\left(hu^2 + \frac{1}{2}gh^2\right) + \partial_y\left(huv\right) = \nu\Big(\partial_x\left(h\partial_x u\right) + \partial_y\left(h\partial_y u\right)\Big)$$

$$-gh\partial_x B - \frac{(\rho_s-\rho_w)}{2\rho}gh^2\partial_x c - \frac{(\rho_0-\rho)(E-D)}{\rho(1-p)}u - fhv - \frac{\tau_{bx}}{\rho} + \frac{\tau_{wx}}{\rho},$$

$$\partial_t(hv) + \partial_x\left(huv\right) + \partial_y\left(hv^2 + \frac{1}{2}gh^2\right) = \nu\Big(\partial_x\left(h\partial_x v\right) + \partial_y\left(h\partial_y v\right)\Big)$$

$$-gh\partial_y B - \frac{(\rho_s-\rho_w)}{2\rho}gh^2\partial_y c - \frac{(\rho_0-\rho)(E-D)}{\rho(1-p)}v + fhu - \frac{\tau_{by}}{\rho} + \frac{\tau_{wy}}{\rho},$$

where

$$\tau_{bx} = \rho C_b u\sqrt{u^2+v^2}, \qquad \tau_{by} = \rho C_b v\sqrt{u^2+v^2},$$

$$\tau_{wx} = \rho C_w w_x\sqrt{w_x^2+w_y^2}, \qquad \tau_{by} = \rho C_w w_y\sqrt{w_x^2+w_y^2}.$$

Equations for Sediment Transport

- Sediment Transport

$$\partial_t(hc) + \partial_x(huc) + \partial_y(hvc) = \kappa\Big(\partial_x(h\partial_x c) + \partial_y(h\partial_y c)\Big) + E - D,$$

- Bed-load morphodynamics

$$(1-p)\,\partial_t B + \partial_x Q_{bx} + \partial_y Q_{by} = \zeta\left(\partial^2_{x^2} B + \partial^2_{y^2} B\right) - \frac{E-D}{1-p}.$$

Empirical Equations

Here, ρ and ρ_0 are respectively, the density of the water- sediment mixture and the density of the saturated bed

$$\rho = \rho_w(1-c) + \rho_s c, \qquad \rho_0 = \rho_w p + \rho_s(1-p).$$

- Deposition of non-cohesive sediments

$$D = w(1-C_a)^m C_a,$$

where w is the settling velocity of a single particle in tranquil water

$$\omega = \frac{\sqrt{(36\nu/d)^2 + 7.5\rho_s g d} - 36\nu/d}{2.8},$$

with ν is the kinematic viscosity of the water, d the averaged diameter of the sediment particle, m an exponent indicating the effects of hindered settling due to high sediment concentrations, C_a the near-bed volumetric sediment concentration, $C_a = \alpha_c c$, where α_c is a coefficient larger than unity. To ensure that the near-bed concentration does not exceed $(1-p)$, the coefficient α_c is computed by

$$\alpha_c = \min\left(2, \frac{1-p}{c}\right).$$

Empirical Equations

- For the entrainment of a cohesive material the following relation is used

$$E = \begin{cases} \varphi \dfrac{\theta - \theta_c}{h} \sqrt{u^2 + v^2} d^{-0.2}, & \text{if } \theta \geq \theta_c, \\ 0, & \text{otherwise,} \end{cases} \tag{1}$$

where φ is a coefficient to control the erosion forces, θ_c is a critical value of Shields parameter for the initiation of sediment motion and θ is the Shields coefficient defined by

$$\theta = \frac{u_*^2}{sgd}, \tag{2}$$

with u_* is the friction velocity defined using the Darcy-Weisbach friction factor f as

$$u_*^2 = \sqrt{\frac{f}{8}} \sqrt{u^2 + v^2}.$$

In (2), s is the submerged specific gravity of sediment given by

$$s = \frac{\rho_s}{\rho_w} - 1.$$

Grass versus Peyer-Peter and Müller Models

Grass fluxes:

$$Q_{bx} = A_g u \left(u^2 + v^2\right)^{\frac{m-1}{2}},$$

$$Q_{by} = A_g v \left(u^2 + v^2\right)^{\frac{m-1}{2}}.$$

Peyer-Peter and Müller fluxes:

$$Q_{bx} = A_p \left(\frac{n_b^2 u \sqrt{u^2 + v^2}}{(s-1) d_{50} h^{\frac{1}{3}}} - 0.047 \right)^{\frac{3}{2}},$$

$$Q_{by} = A_p \left(\frac{n_b^2 v \sqrt{u^2 + v^2}}{(s-1) d_{50} h^{\frac{1}{3}}} - 0.047 \right)^{\frac{3}{2}},$$

where $A_p = 8\sqrt{g s d_{50}^3}$, with d_{50} is the median diameter of the sediment and the grain specific gravity $s = \frac{\rho_s}{\rho_w} - 1$.

Scaling procedures

We consider the one-dimensional sediment transport equations

$$\begin{aligned}
\partial_t h + \partial_x(hu) &= 0, \\
\partial_t(hu) + \partial_x\left(hu^2 + \frac{1}{2}gh^2\right) &= -gh\partial_x B - \frac{(\rho_s - \rho_w)}{2\rho}gh^2\partial_x c, \\
\partial_t(hc) + \partial_x(huc) &= 0, \\
(1-p)\partial_t B + \partial_x\left(Au|u|^{m-1}\right) &= 0.
\end{aligned}$$

The associated eigenvalues are

$$\lambda_1 = 2\sqrt{-Q}\cos\left(\frac{1}{3}\theta\right) + \frac{2}{3}u, \qquad \lambda_2 = 2\sqrt{-Q}\cos\left(\frac{1}{3}(\theta + 2\pi)\right) + \frac{2}{3}u,$$

$$\lambda_3 = 2\sqrt{-Q}\cos\left(\frac{1}{3}(\theta + 4\pi)\right) + \frac{2}{3}u, \qquad \lambda_4 = u,$$

where $d = \frac{1}{(1-p)h}Am|u|^{m-1}$ and $\theta = \arccos\left(\frac{R}{\sqrt{-Q^3}}\right)$, with

$$Q = -\frac{1}{9}\left(u^2 + 3g(h+d)\right), \qquad R = \frac{u}{54}\left(9g(2h-d) - 2u^2\right).$$

Scaling procedures

Scaling the time and space using special reference values for water height, water velocity and bed-load, the governing sediment transport equations can be reformulated in dimensionless as:

$$\begin{aligned}
\epsilon\partial_t h + \partial_x(hu) &= 0, \\
\epsilon\partial_t(hu) + \partial_x\left(hu^2 + \frac{1}{2Fr^2}h^2\right) &= -\frac{1}{2Fr^2}h\partial_x B - \frac{(\rho_s-\rho_w)}{4\rho Fr^2}h^2\partial_x c, \\
\epsilon\partial_t(hc) + \partial_x(huc) &= 0, \\
(1-p)\partial_t B + \partial_x\left(u|u|^{m-1}\right) &= 0.
\end{aligned}$$

where $\epsilon = \dfrac{A|u_{ref}|^{m-1}}{h_{ref}}$, $Fr = \dfrac{u_{ref}}{\sqrt{gh_{ref}}}$.

- ▷▷▷ Typical values of ϵ are 10^{-3} to 10^{-6}.
- ▷▷▷ Typical values of Fr are 0.9 to 0.01.

II. Numerical Method

Equations in Conservative Form

$$\partial_t \mathbf{W} + \partial_x \left(\mathbf{F}(\mathbf{W}) - \tilde{\mathbf{F}}(\mathbf{W}) \right) + \partial_y \left(\mathbf{G}(\mathbf{W}) - \tilde{\mathbf{G}}(\mathbf{W}) \right) = \mathbf{S}(\mathbf{W}) + \mathbf{Q}(\mathbf{W}),$$

where

$$\mathbf{W} = \begin{pmatrix} h \\ hu \\ hv \\ hc \\ (1-p)B \end{pmatrix}, \mathbf{S}(\mathbf{W}) = \begin{pmatrix} 0 \\ -gh\partial_x B - \frac{(\rho_s - \rho_w)}{2\rho} gh^2 \partial_x c \\ -gh\partial_y B - \frac{(\rho_s - \rho_w)}{2\rho} gh^2 \partial_y c \\ 0 \\ 0 \end{pmatrix}, \tilde{\mathbf{F}}(\mathbf{W}) = \begin{pmatrix} 0 \\ \nu \partial_x (hu) \\ \nu \partial_x (hv) \\ \kappa \partial_x (hc) \\ \zeta \partial_x B \end{pmatrix}$$

$$\mathbf{F}(\mathbf{W}) = \begin{pmatrix} hu \\ hu^2 + \frac{1}{2} gh^2 \\ huv \\ huc \\ Au \left(u^2 + v^2\right)^{\frac{m-1}{2}} \end{pmatrix}, \mathbf{G}(\mathbf{W}) = \begin{pmatrix} hv \\ huv \\ hv^2 + \frac{1}{2} gh^2 \\ hvc \\ Av \left(u^2 + v^2\right)^{\frac{m-1}{2}} \end{pmatrix}, \tilde{\mathbf{G}}(\mathbf{W}) = \begin{pmatrix} 0 \\ \nu \partial_y (hu) \\ \nu \partial_y (hv) \\ \kappa \partial_y (hc) \\ \zeta \partial_y B \end{pmatrix}$$

Formulation of the Method

The integral form of the shallow water equations over a fixed volume V is given by

$$\partial_t \int_V \mathbf{W}\, dV + \int_V \left(\partial_x \left(\mathbf{F}(\mathbf{W}) - \tilde{\mathbf{F}}(\mathbf{W})\right) + \partial_y \left(\mathbf{G}(\mathbf{W}) - \tilde{\mathbf{G}}(\mathbf{W})\right)\right) dV = \int_V \mathbf{S}(\mathbf{W})\, dV,$$

that, using divergence theorem for the second integral leads to

$$\partial_t \int_V \mathbf{W}\, dV + \int_{\partial V} \mathcal{F}(\mathbf{W};\mathbf{n})\, d\sigma - \int_{\partial V} \tilde{\mathcal{F}}(\mathbf{W};\mathbf{n})\, d\sigma = \int_V \mathbf{S}(\mathbf{W})\, dV,$$

where

$$\mathcal{F}(\mathbf{W};\mathbf{n}) = \mathbf{F}(\mathbf{W})n_x + \mathbf{G}(\mathbf{W})n_y, \qquad \tilde{\mathcal{F}}(\mathbf{W};\mathbf{n}) = \tilde{\mathbf{F}}(\mathbf{W})n_x + \tilde{\mathbf{G}}(\mathbf{W})n_y.$$

and ∂V is the surface surrounding the volume V. Here, $\mathbf{n} = (n_x, n_y)^T$ denotes the unit outward normal to the surface ∂V.

The SRNH scheme uses:

- Finite volume method for spatial discretization
- Two-step Runge-Kutta scheme for time integration
- Well-balanced treatment of the source terms
- Second-order MUSCL reconstruction with slope limiters
- Centered-vertex method for diffusion operators

Finite Volume Discretization

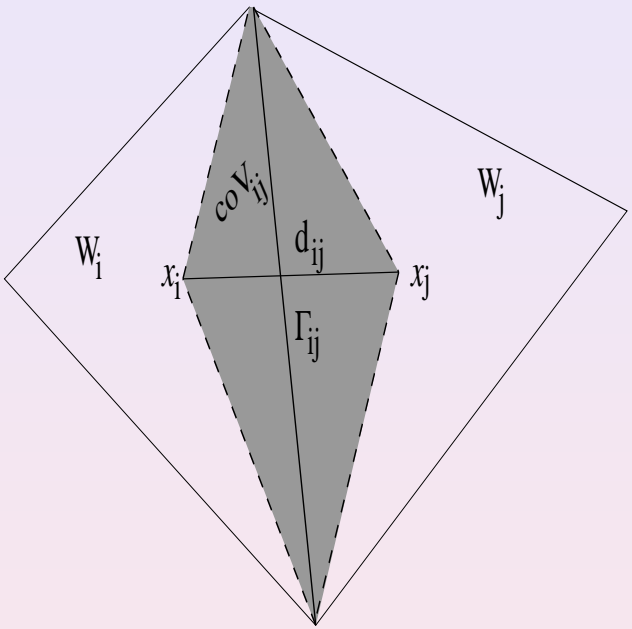

$$\mathbf{W}_i = \frac{1}{|\mathcal{T}_i|}\int_{\mathcal{T}_i} \mathbf{W}\, dV,$$

$$\begin{aligned}\mathbf{W}_i^{n+1} &= \mathbf{W}_i^n - \frac{\Delta t}{|\mathcal{T}_i|}\sum_{j\in N(i)}\int_{\Gamma_{ij}} \mathcal{F}(\mathbf{W}^n;\mathbf{n})\, d\sigma + \\ &\frac{\Delta t}{|\mathcal{T}_i|}\sum_{j\in N(i)}\int_{\Gamma_{ij}} \tilde{\mathcal{F}}(\mathbf{W}^n;\mathbf{n})\, d\sigma - \\ &\frac{\Delta t}{|\mathcal{T}_i|}\int_{\mathcal{T}_i} \mathbf{S}(\mathbf{W})^n\, dV,\end{aligned}$$

$$\int_{\Gamma_{ij}} \mathcal{F}(\mathbf{W};\mathbf{n})\, d\sigma = \Phi\left(\mathbf{W}_i, \mathbf{W}_j, S_{ij}, \mathbf{n}_{ij}\right)\left|\Gamma_{ij}\right|.$$

The SRNH Scheme consists of a predictor and corrector stages given as:

$$\begin{aligned}\mathbf{W}_{ij}^n &= \frac{1}{2}\left(\mathbf{W}_i^n + \mathbf{W}_j^n\right) - \frac{\alpha_{ij}^n}{2S_{ij}^n}\left(\mathcal{F}\left(\mathbf{W}_j^n;\mathbf{n}_{ij}\right) - \mathcal{F}\left(\mathbf{W}_i^n;\mathbf{n}_{ij}\right)\right) + \frac{\alpha_{ij}^n}{2S_{ij}^n}\mathbf{S}_{ij}^n, \\ \mathbf{W}_i^{n+1} &= \mathbf{W}_i^n - \frac{\Delta t}{|\mathcal{T}_i|}\sum_{j\in N(i)}\Phi\left(\mathbf{W}_i, \mathbf{W}_j, S_{ij}, \mathbf{n}_{ij}\right)\left|\Gamma_{ij}\right| + \Delta t\mathbf{S}_i^n,\end{aligned}$$

with $\Phi\left(\mathbf{W}_i, \mathbf{W}_j, S_{ij}, \mathbf{n}_{ij}\right) = \mathcal{F}\left(\mathbf{W}_{ij}^n;\mathbf{n}_{ij}\right), \qquad S_{ij}^n = \max_p\left(\left|\lambda_{p,i}^n\right|, \left|\lambda_{p,j}^n\right|\right).$

Time Integration

To deal with the source terms $\mathbf{Q}$, a standard splitting procedure is employed for the discrete system as

$$\begin{aligned}
\mathbf{W}_{ij}^{n} &= \frac{1}{2}\left(\mathbf{W}_{i}^{n}+\mathbf{W}_{j}^{n}\right)-\frac{1}{2}\operatorname{sgn}\left[\mathbf{A}_{\eta}\left(\overline{\mathbf{W}}\right)\right]\left(\mathbf{W}_{j}^{n}-\mathbf{W}_{i}^{n}\right), \\
\mathbf{W}_{i}^{*} &= \mathbf{W}_{i}^{n}-\frac{\Delta t}{|\mathcal{T}_{i}|}\sum_{j\in N(i)}\mathcal{F}\left(\mathbf{W}_{ij}^{n};\eta_{ij}\right)|\Gamma_{ij}|+\Delta t\mathbf{S}\left(\mathbf{W}_{i}^{n}\right), \\
\mathbf{W}_{i}^{n+1} &= \mathbf{W}_{i}^{*}+\Delta t\mathbf{Q}\left(\mathbf{W}_{i}^{*}\right),
\end{aligned}$$

where the sign matrix is defined as

$$\operatorname{sgn}\left[\mathbf{A}_{\eta}\left(\overline{\mathbf{W}}\right)\right]=\mathcal{R}(\overline{\mathbf{W}})\operatorname{sgn}\left[\Lambda(\overline{\mathbf{W}})\right]\mathcal{R}^{-1}(\overline{\mathbf{W}}),$$

with $\Lambda(\overline{\mathbf{W}})$ is the diagonal matrix of eigenvalues, $\mathcal{R}(\overline{\mathbf{W}})$ is the right eigenvector matrix and $\overline{\mathbf{W}}$ is the Roe's average state.

Adaptation Procedure

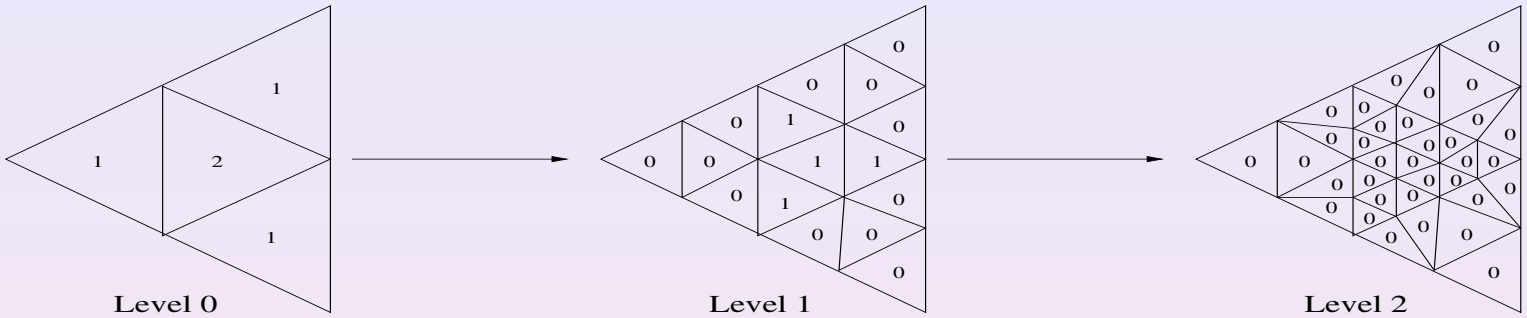

In our simulations, the adaption criterion is based on the normalized bed-load, and is evaluated as

$$Crit^n(\mathcal{T}_i) = \frac{B(\mathcal{T}_i)}{\max\limits_{\mathcal{T}_j} B(\mathcal{T}_j)},$$

where $B(\mathcal{T}_i)$ is the bed-load on cell $\mathcal{T}_i$. Hence, an adaptation procedure can be performed as follows:
Given a sequence of three real numbers $\{r_m\}$ such that
$0 = r_0 < r_1 < r_2 < r_3 < r_4 = 1$. If a macro-element $\mathcal{T}_i$ satisfies the condition

$$r_m \leq Crit^n(\mathcal{T}_i) \leq r_{m+1}, \qquad m = 0, \ldots, 3.$$

then $\mathcal{T}_i$ is divided into 4^m triangles.

III. Numerical Results and Applications

Some References


E. Audusse, F. Benkhaldoun, S. Sari, M. Seaid, P. Tassi. *A fast finite volume solver for multi-layered shallow water flows with mass exchange*, (2014) *J. Comp. Physics*. Vol 272, pp:23-45


F. Benkhaldoun, I. Elmahi, S. Sari, M. Seaid. *An unstructured finite volume method for coupled models of suspended sediment and bed-load transport in shallow water flows*, (2013) *Int. J. Num. Meth. Fluids*. Vol 72, pp:976-993


F. Benkhaldoun, S. Sari, M. Seaid. *A flux-limiter method for dam-break flows over erodible sediment beds*, (2012) *Applied Mathematical Modelling*. Vol 36, pp:4847-4861


F. Benkhaldoun, S. Daoudi, I. Elmahi, M. Seaid. *Numerical modelling of sediment transport in the Nador lagoon (Morocco)*, (2012) *Appl. Numer. Math*. Vol 62, pp:1749-1766


F. Benkhaldoun, S. Sahmim, M. Seaid. *Mathematical development and verification of a finite volume model for morphodynamic flow applications*, (2011) *Advances in Applied Mathematics and Mechanics*. Vol 3, pp:470-492


F. Benkhaldoun, I. Elmahi, M. Seaid. *A new finite volume method for flux-gradient and source-term balancing in shallow water equations*, (2010) *Computer Methods in Applied Mechanics and Engineering*. Vol 199, pp:49-52


F. Benkhaldoun, S. Sahmim, M. Seaid. *A two-dimensional finite volume morphodynamic model on unstructured triangular grids*, (2010) *Int. J. Num. Meth. Fluids*. Vol 63, pp:1296-1327


F. Benkhaldoun, S. Sahmim, M. Seaid. *Solution of the Sediment Transport Equations using a Finite Volume Method based on Sign Matrix*, (2009) *SIAM J. Sci. Comp*. Vol 31, pp:2866-2889

Verification of C-property

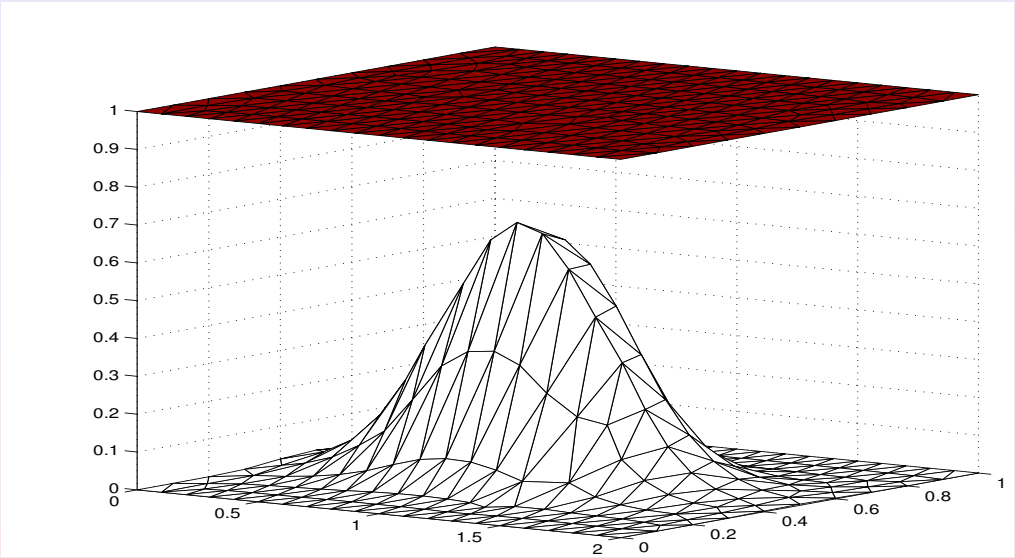

	Minmod limiter			VanAlbada limiter		
Mesh	$t = 0.2\ s$	$t = 1\ s$	$t = 10\ s$	$t = 0.2\ s$	$t = 1\ s$	$t = 10\ s$
25×10	0E-00	5.148E-19	1.243E-17	1.210E-18	7.780E-18	4.101E-17
50×20	1.050E-19	3.560E-19	1.180E-17	7.681E-19	5.666E-18	3.170E-17
100×40	1.380E-20	3.050E-19	6.541E-18	5.871E-19	4.520E-18	3.050E-17

Verification of Mesh Adaptation

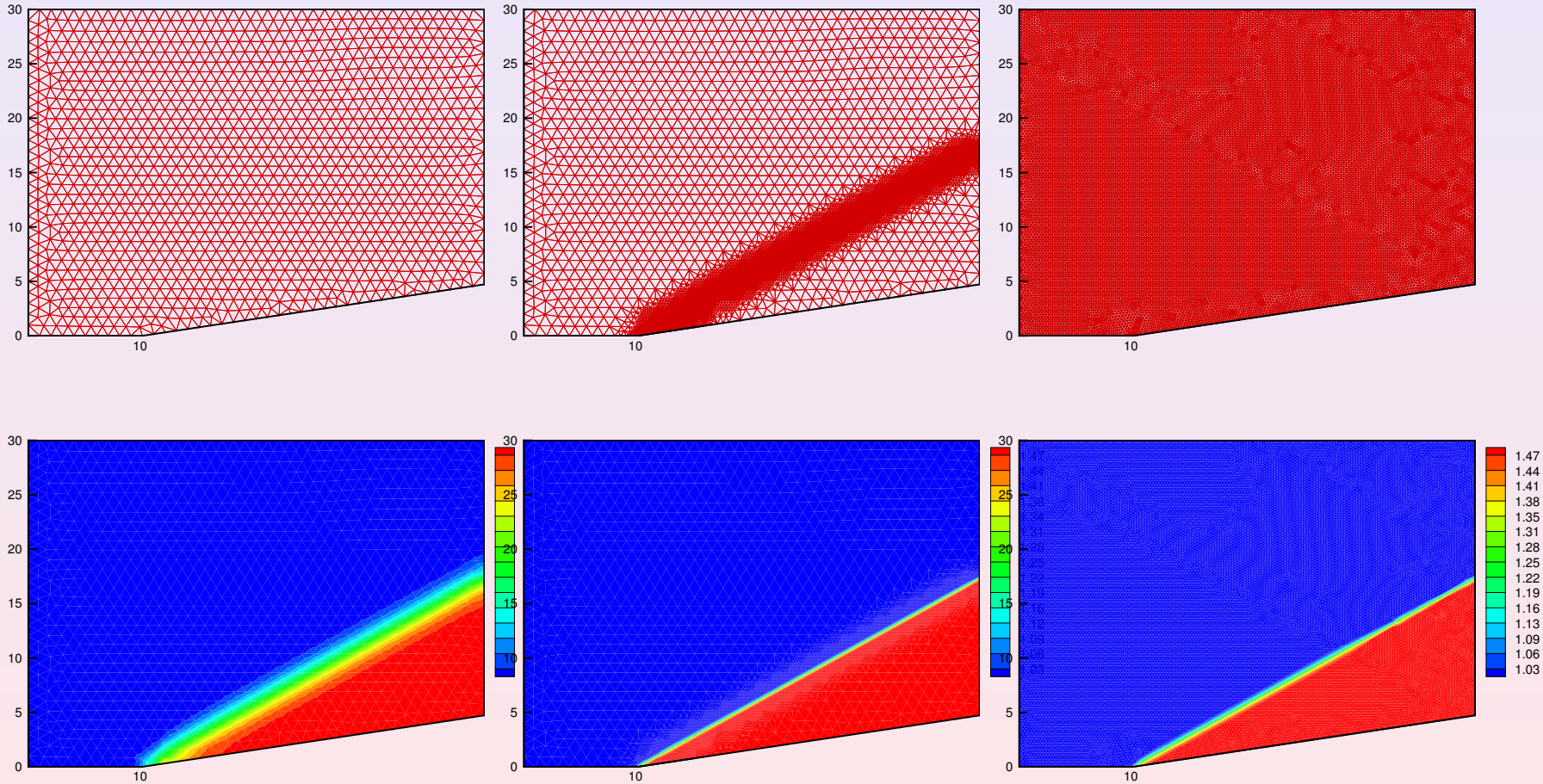

Verification of Mesh Adaptation

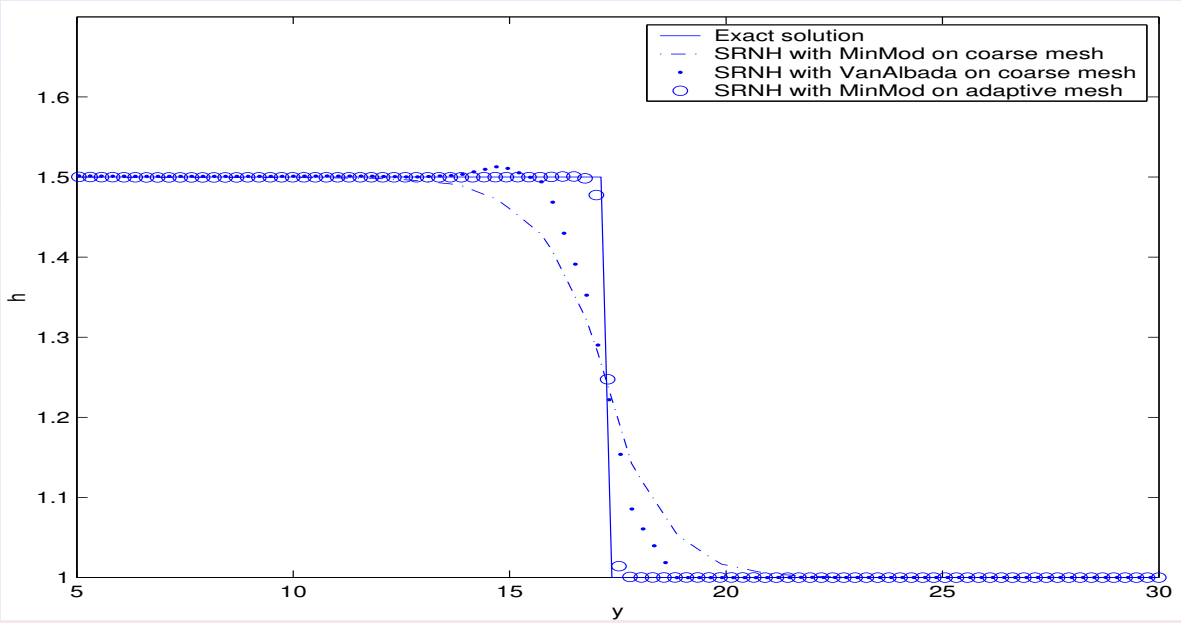

	# of elements	# of nodes	Maximum of h	Deflection angle	CPU time
Coarse	2521	1329	1.50048	9.661°	0.80
Adaptive	16269	8234	1.50273	9.011°	7.50
Fine	40864	20705	1.50246	9.031°	17.30

Comparison to Experiments

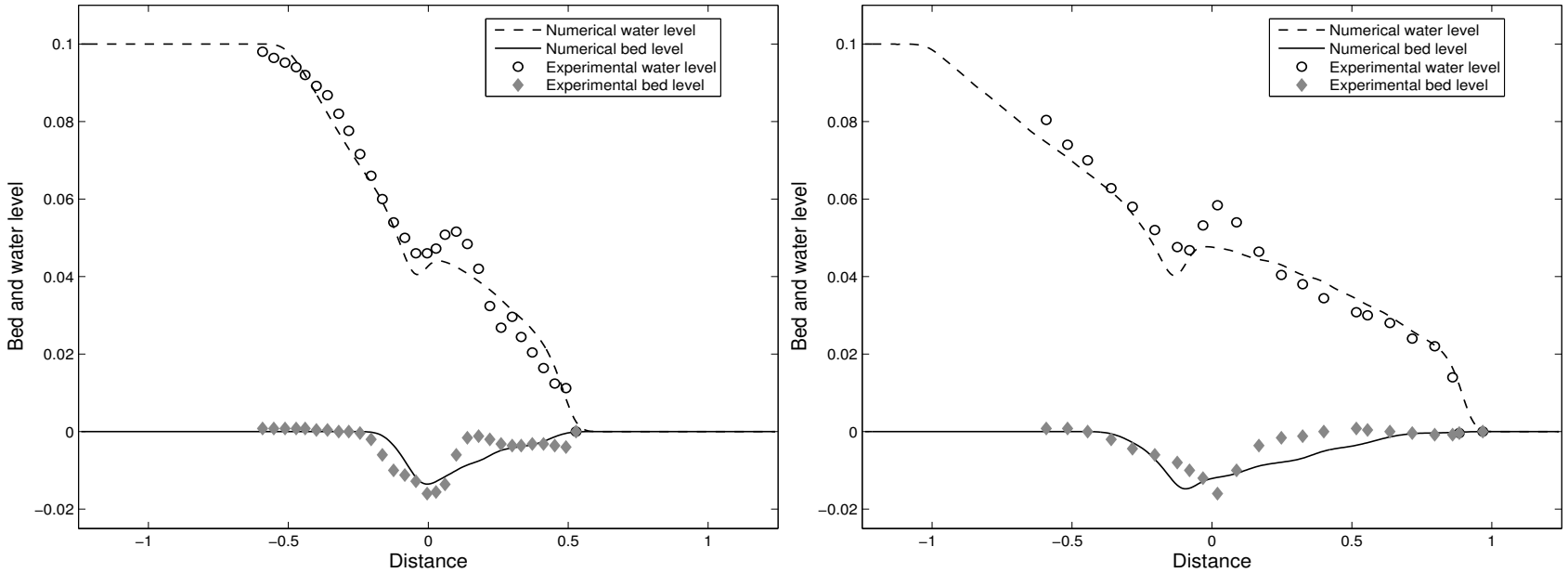

Single-layer versus multi-layer beds

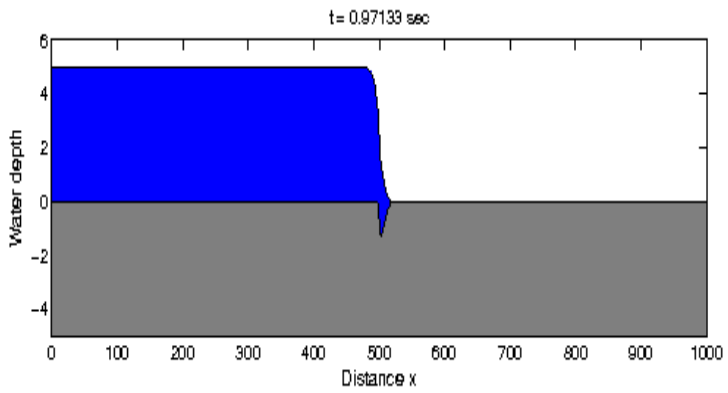

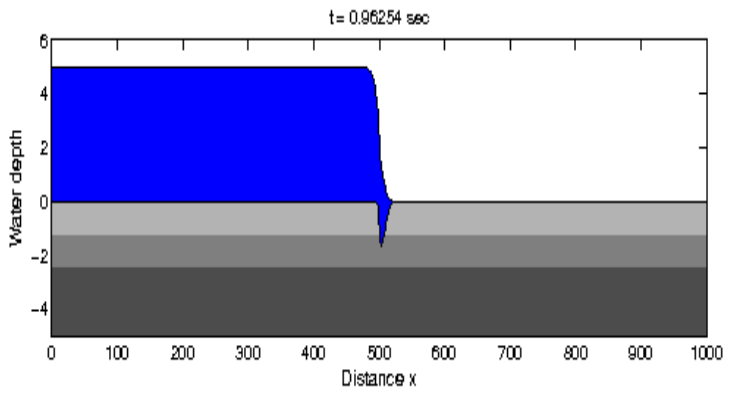

Grass versus Peyer-Peter and Müller Models

Grass fluxes:

$$Q_{bx} = A_g u \left(u^2 + v^2\right)^{\frac{m-1}{2}},$$

$$Q_{by} = A_g v \left(u^2 + v^2\right)^{\frac{m-1}{2}}.$$

Peyer-Peter and Müller fluxes:

$$Q_{bx} = A_p \left(\frac{n_b^2 u \sqrt{u^2 + v^2}}{(s-1) d_{50} h^{\frac{1}{3}}} - 0.047 \right)^{\frac{3}{2}},$$

$$Q_{by} = A_p \left(\frac{n_b^2 v \sqrt{u^2 + v^2}}{(s-1) d_{50} h^{\frac{1}{3}}} - 0.047 \right)^{\frac{3}{2}},$$

where $A_p = 8\sqrt{g(s-1)d_{50}^3}$, with d_{50} is the median diameter of the sediment and the grain specific gravity $s = \frac{\rho_s}{\rho_w}$.

Grass Results

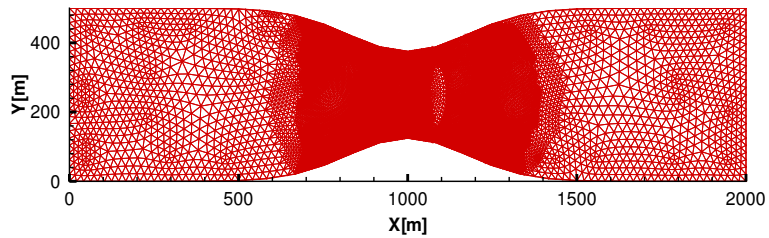

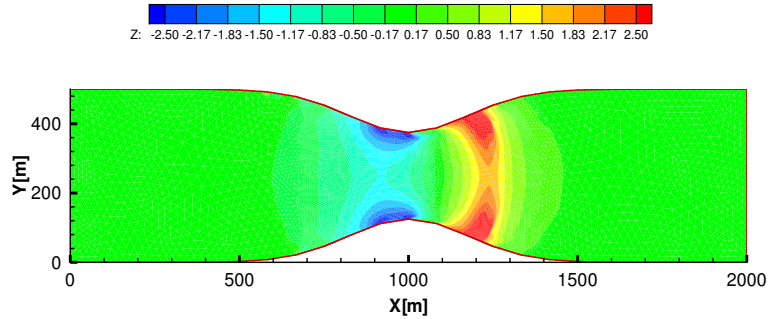

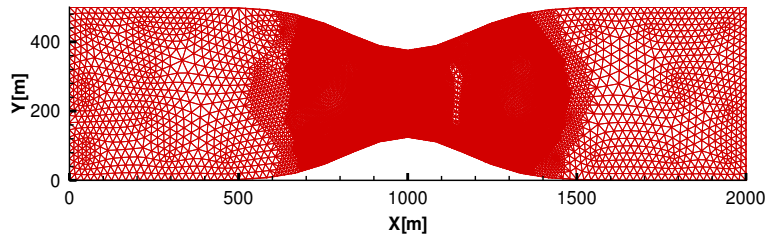

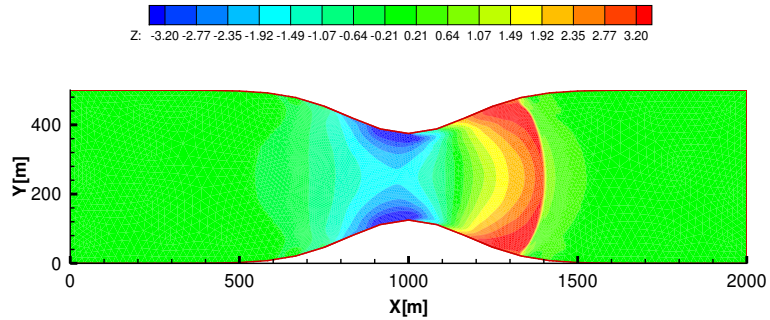

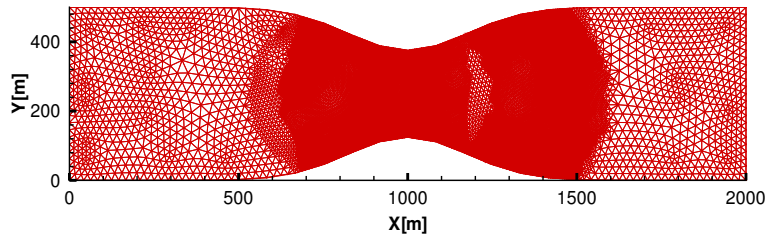

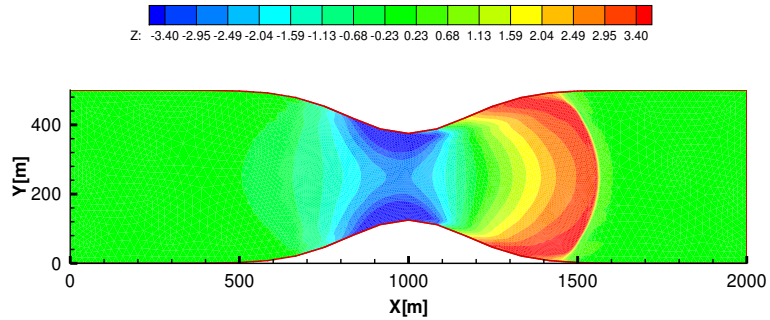

Peyer-Peter and Müller Results

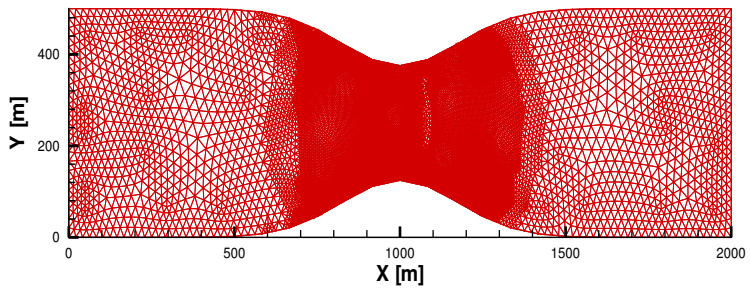

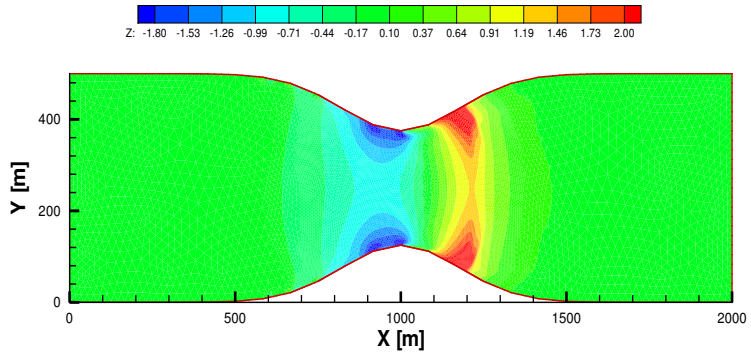

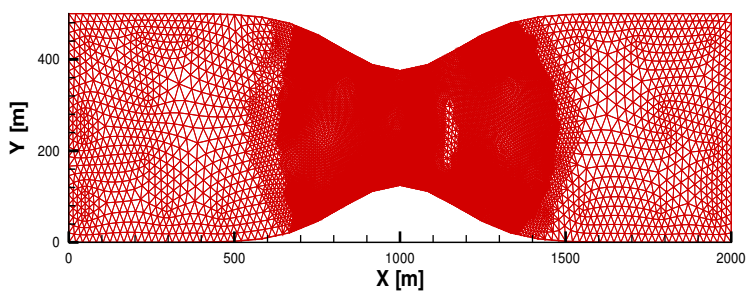

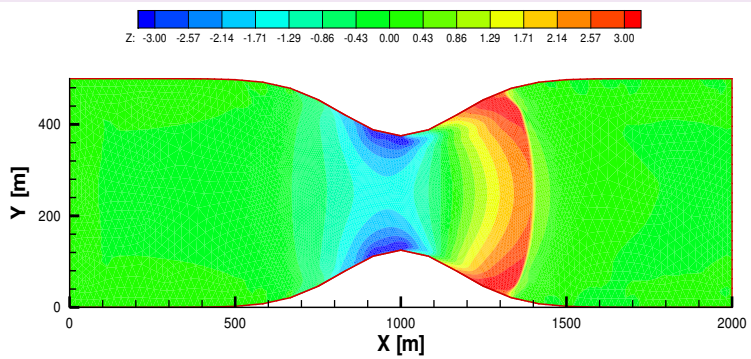

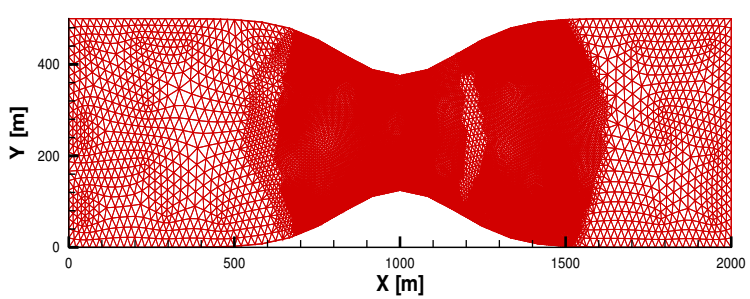

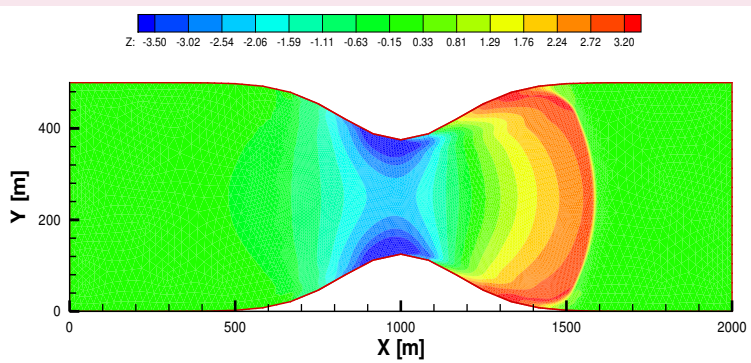

Grass versus Peyer-Peter and Müller Models

	Grass model			Meyer-Peter and Müller model		
	$t = 25\ h$	$t = 50\ h$	$t = 100\ h$	$t = 25\ h$	$t = 50\ h$	$t = 100\ h$
# of elements	22125	25772	29284	21490	25895	30029
# of nodes	11309	13144	14913	10991	13203	15288
Maximum of Z	4.08	4.20	4.50	3.20	4.05	4.20
Minimum of Z	-3.71	-5.59	-7.46	-2.80	-4.55	-6.30
CPU time	309	646	870	397	730	1273

Dam-break over Erodible Bed

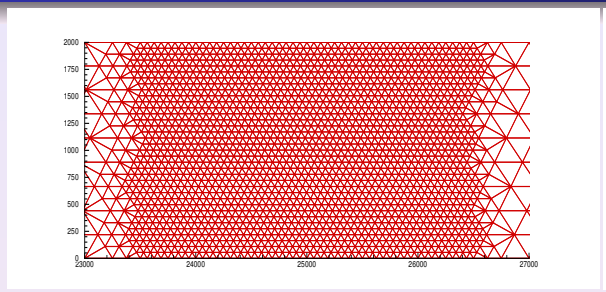
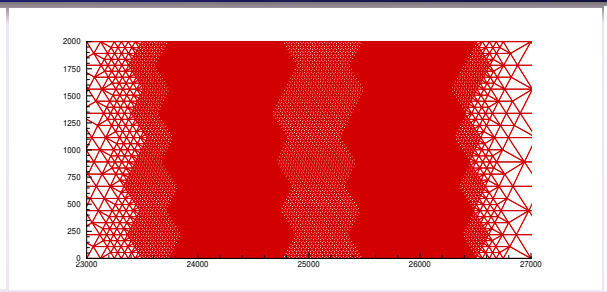
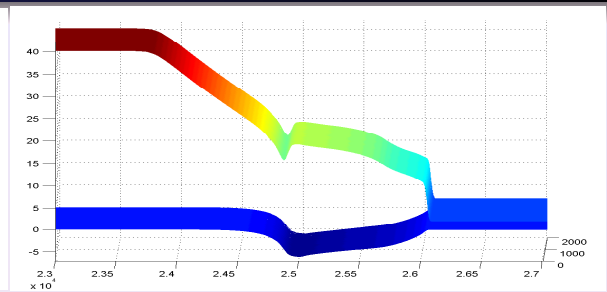
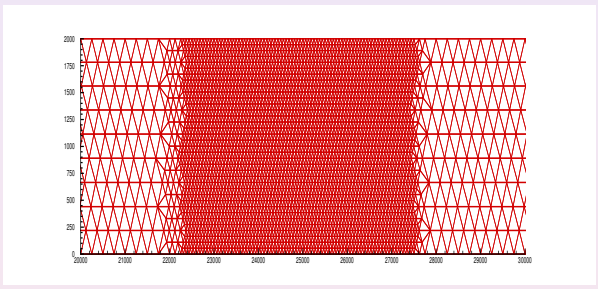
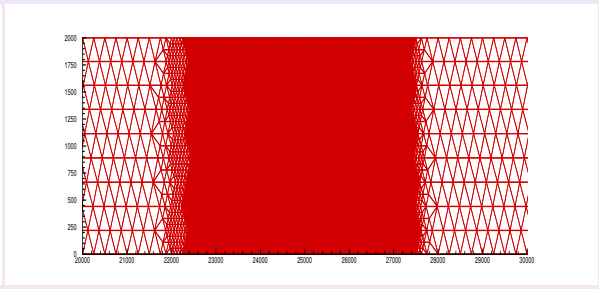
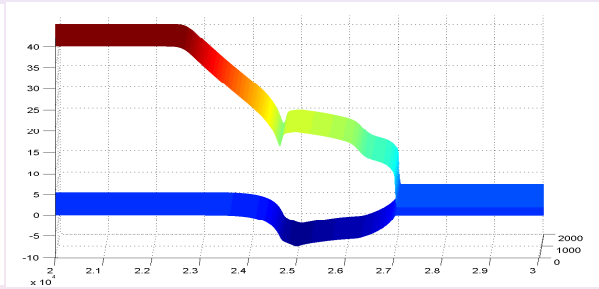
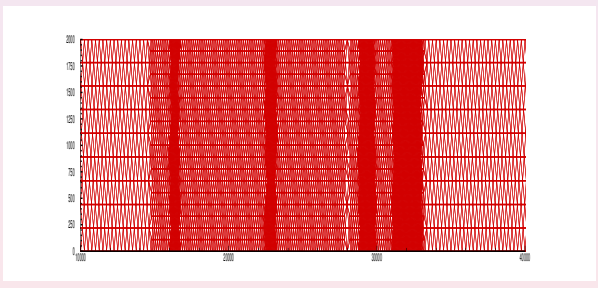
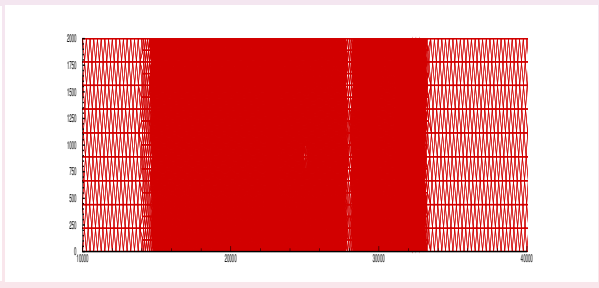
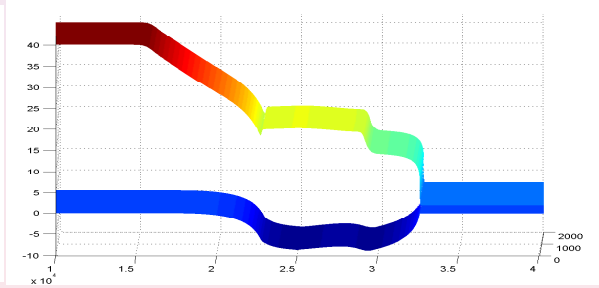
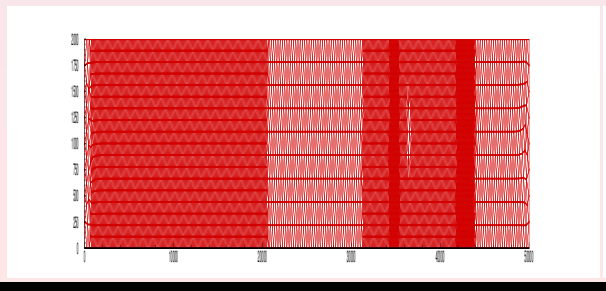
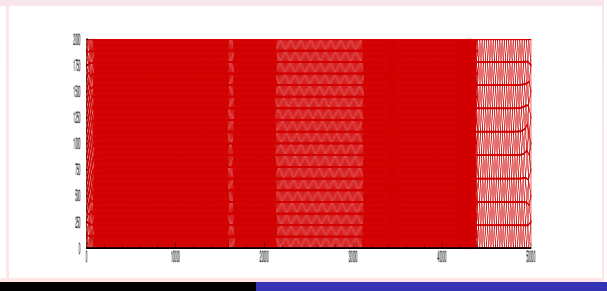
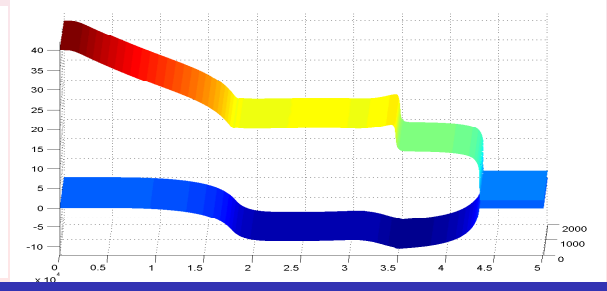

Partial Dam-break over Fixed Bed

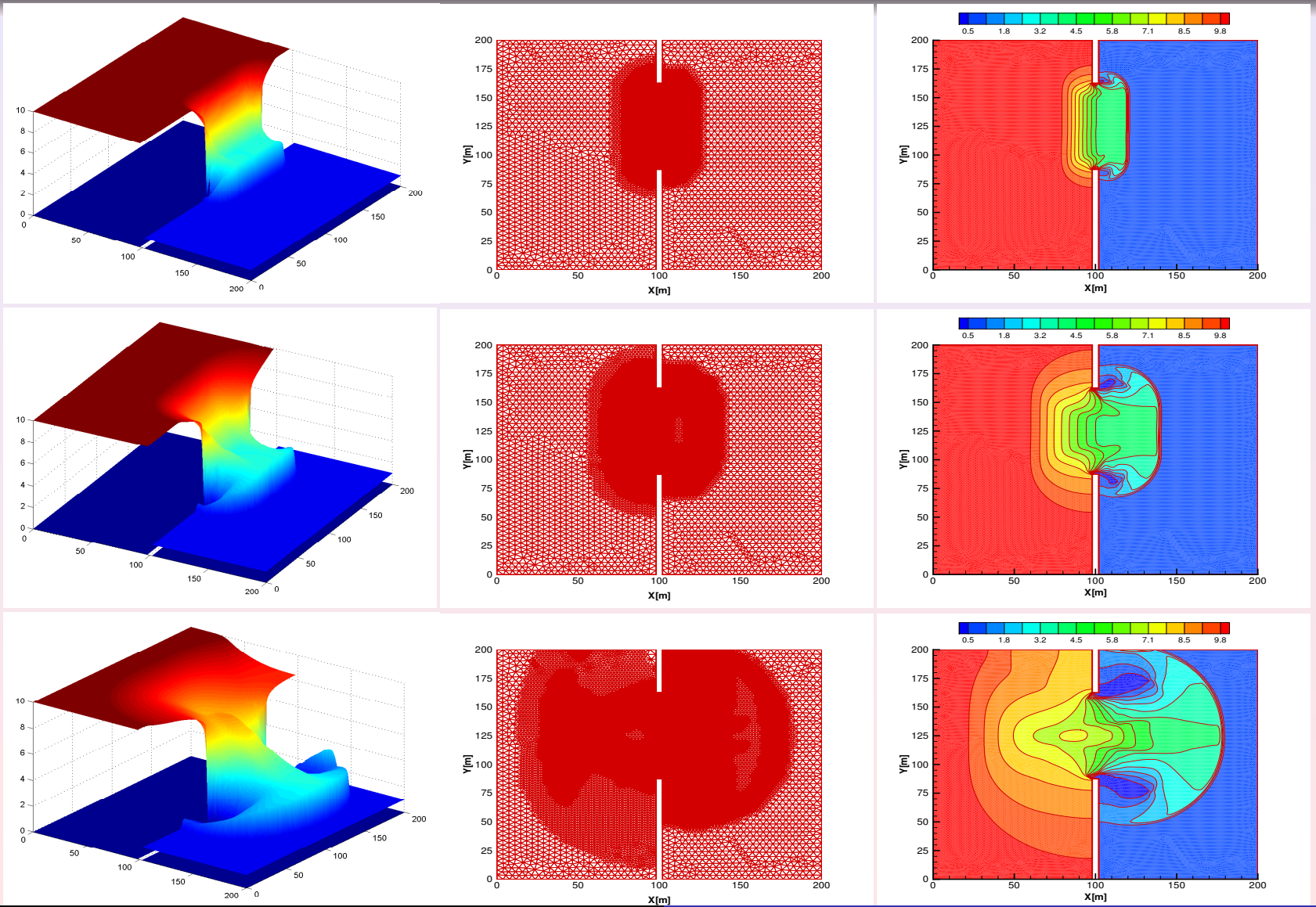

Partial Dam-break over Erodible Bed

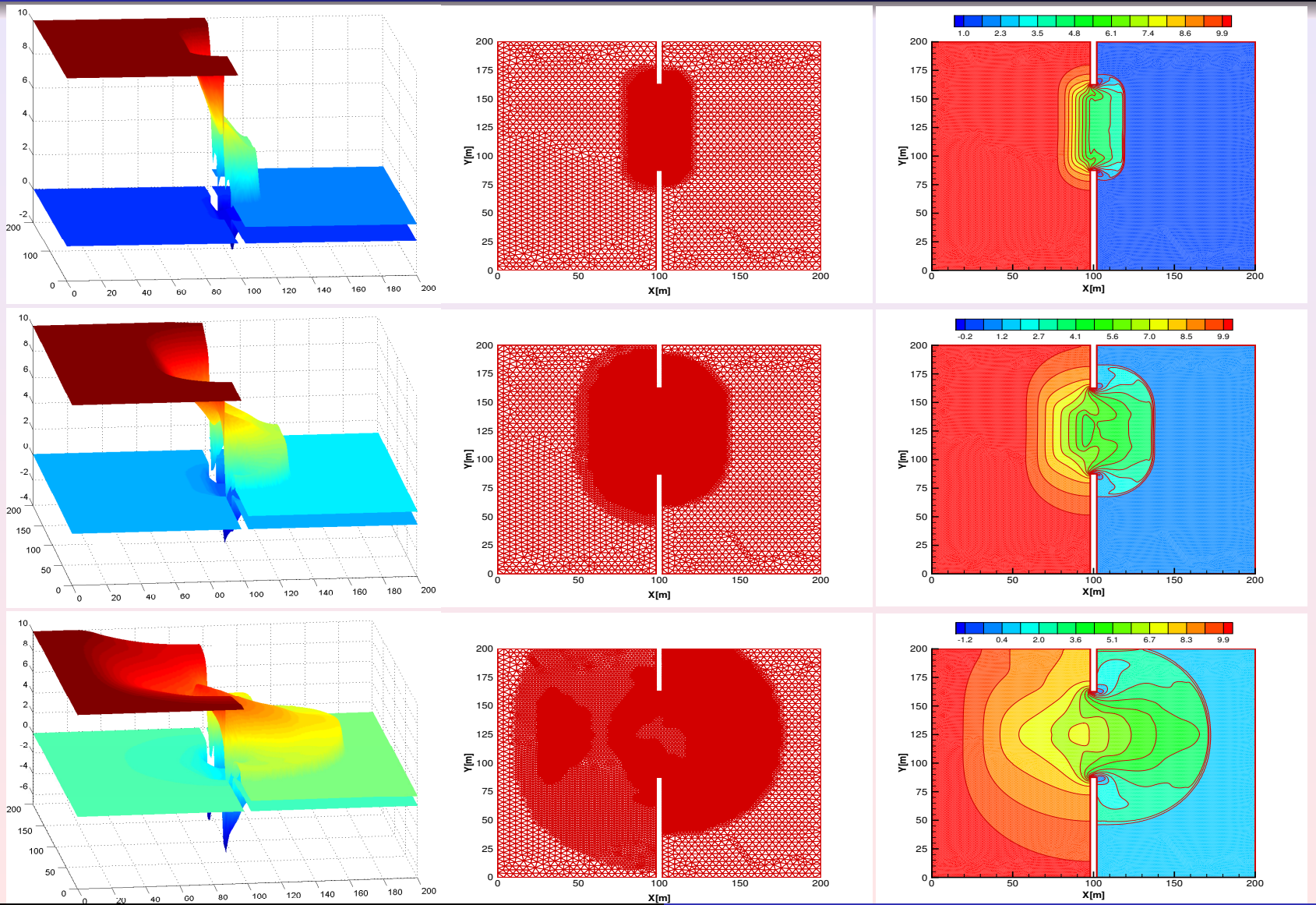

Suspended sediment in the Nador lagoon

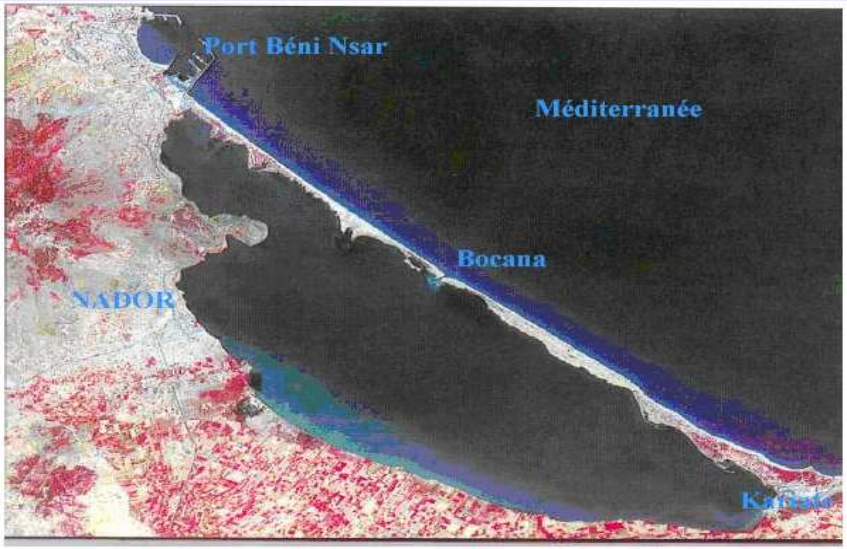

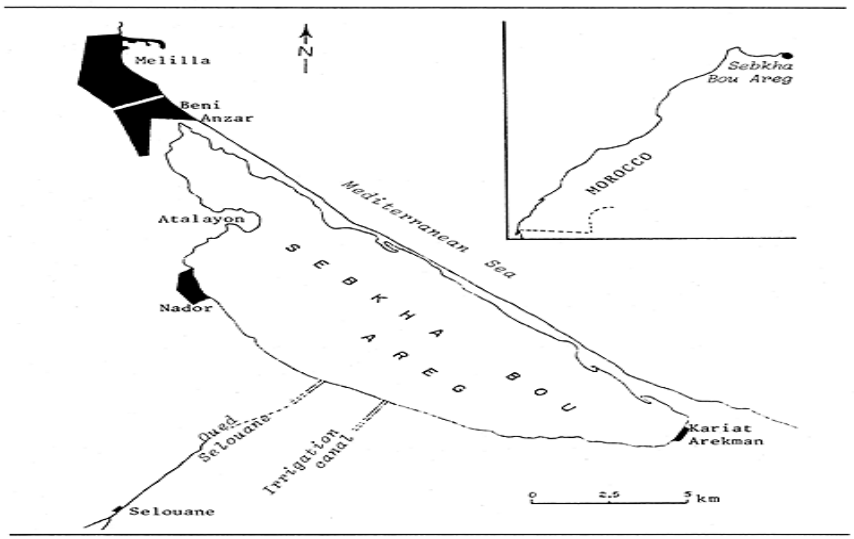

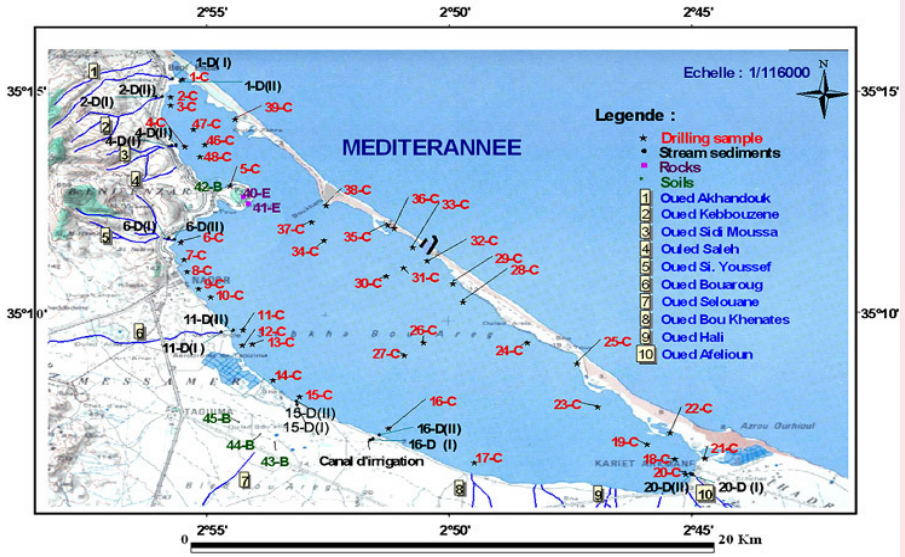

Suspended sediment in the Nador lagoon

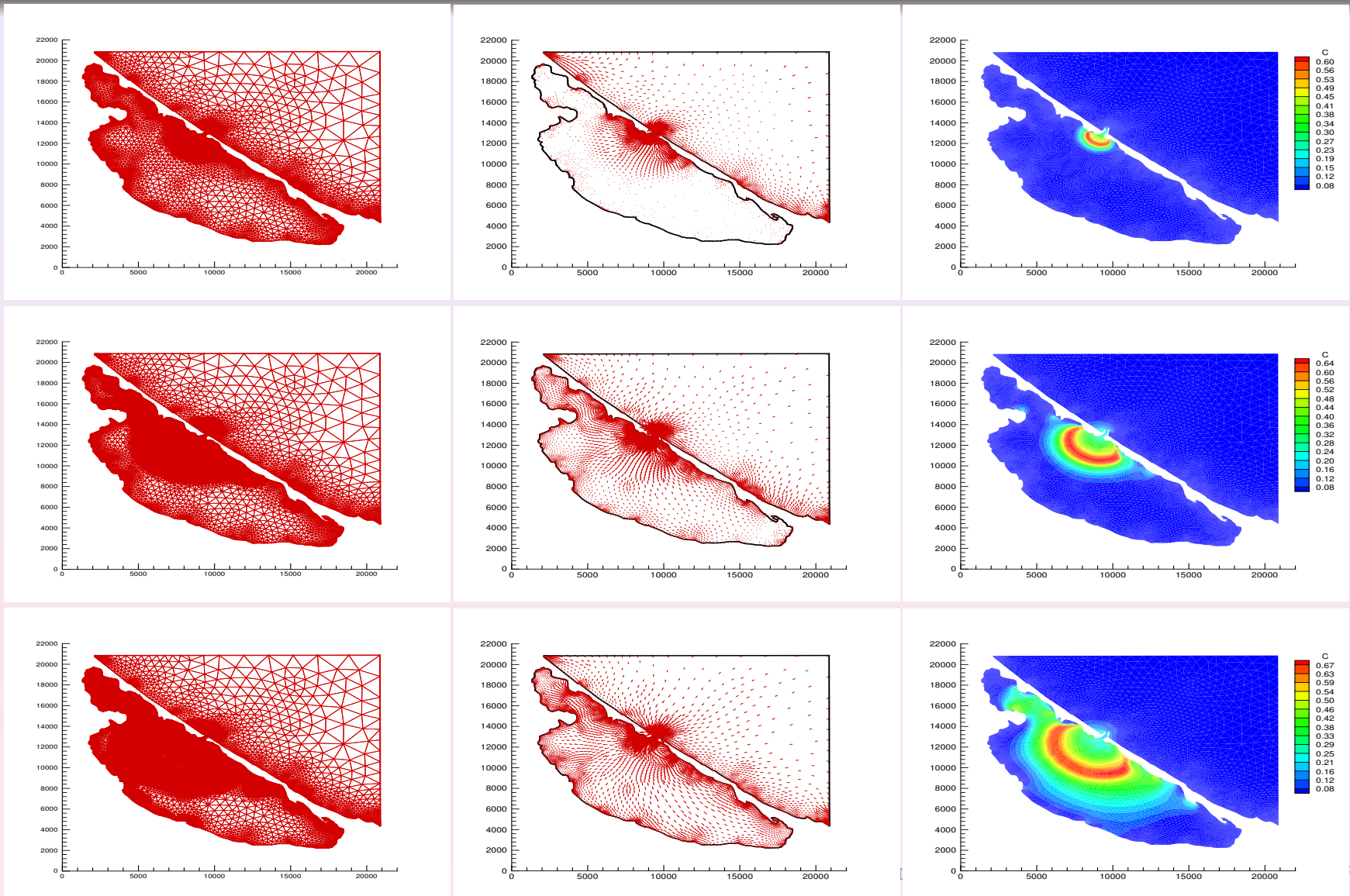

Suspended sediment in the Nador lagoon

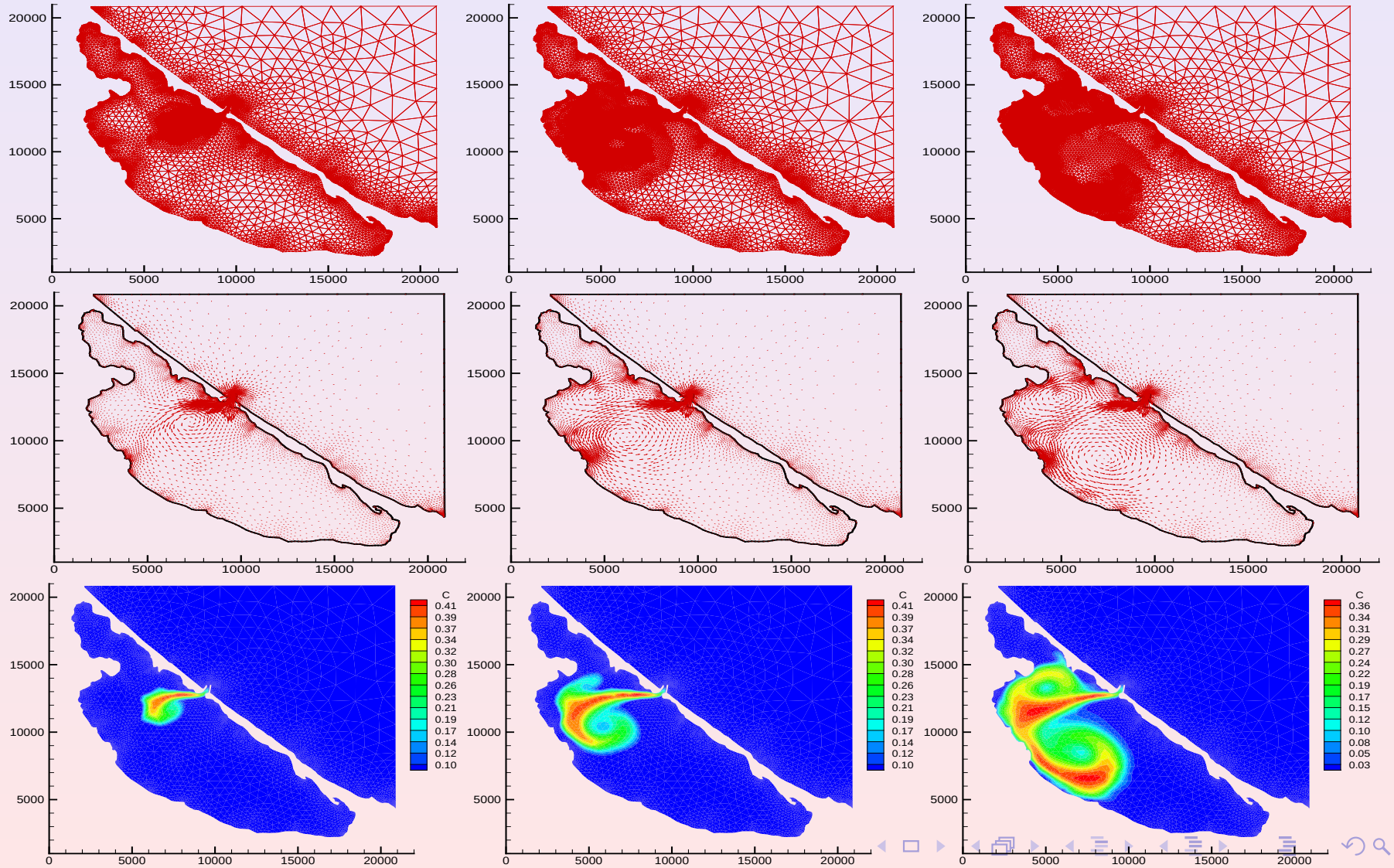

Outlook

- It has been shown that combining shallow water equations and sediment transport is an accurate mathematical tools for modeling morphodynamical problems. The combined model accurately resolves the space scales formed in both the hydrodynamic and the morphodynamics.
- Concerning the numerical method, the proposed finite volume scheme has exhibited many desirable properties for morphodynamical problems such as: (i) Accurate prediction of both, the free surface and the bed-load with correct C-property, (ii) stable representation of free surface response to the movable bed, and (iii) good convergence behaviors with respect to computational refinement and high efficiency compared with computations on fixed meshes.
- Open questions:
  - Reconstruction of asymptotic-preserving schemes to resolve different time scales.
  - Development of an efficient criteria for mesh adaptation.
  - Quantifying the uncertainty in the inputs parameters.

Thank you.